SIMULATION AND EXPERIMENTAL INVESTIGATORS ON RECTANGULAR, CIRCULAR AND CYLINDRICAL DIELECTRIC RESONATOR ANTENNA

S. Sreekantan, Y. K. Ling, and Z. A. Ahmad

School of Materials and Mineral Resources Engineering
Universiti Sains Malaysia
Nibong Tebal, Pulau Pinang 14300, Malaysia

M. F. Ain, M. B. Othman, and S. I. S. Hassan

School of Electrical and Electronic Engineering
Universiti Sains Malaysia
Nibong Tebal, Pulau Pinang 14300, Malaysia

Abstract—In this paper, theoretical and simulation studies on rectangular and annular dielectric resonator antenna (DRA) made of TiO_2 was reported. The ceramic was fabricated by solid state reaction at $1200°C$. The structural and dielectric properties were investigated by X-Ray Diffraction (XRD), Field Emission Electron Microscopy (FESEM) and network Analyzer. The XRD results showed the presence of rutile phase and the microstructure comprised of fine grain (0.2–$0.5\,\mu m$) and large grain 1.0–$1.5\,\mu m$. The rectangular and annular shape TiO_2 DRA with high dielectric constant ($\varepsilon = 84$) and low loss tangent (0.080) were fed with $50\,\Omega$ microstrip transmission line and comparision between the various shape were investigated. The return loss, input impedance and radiation pattern TiO_2 DRA was studied. Design simulation results using CST Microwave Studio 2008 also was presented.

1. INTRODUCTION

In the technology driven global market today, communication devices have become part and parcel of our routine life. The ongoing drive for communication devices miniaturization has force the necessity to reduce the size of available materials and also to discover alternative

Corresponding author: S. Sreekantan (srimala@eng.usm.my).

materials. Lately, DRA has been seen as an alternative material for communication devices due to their attractive features [1–3]. A DRA can be fabricated in various shape such as rectangular, cylindrical, hemispherical and other geometries which allows more flexibility in antenna design [4–10]. Furthermore, DRA can be excited by various feed mechanism from probe, slot, microstrip, coplanar lines and waveguide slot [11–15]. These excitation mechanisms can accommodate a variety of design requirements. Besides that, DRA have other advantages such as light weight, small size, low profile, high radiation efficiency and low profile [11]. However, DRA is found to have a limited bandwidth associated to the resonant nature. One of the simple approaches to overcome the drawback is to use ceramic materials with high dielectric value.

In our previous work, we have reported the structural and antenna performance of the cylindrical DRA made of TiO_2. We observed that the input impedance of the cylindrical DRA by simulation using CST software closely matches with the experimental study. However, measured bandwidth is only 14.28% of the simulated bandwidth. The E-plane and H-plane radiation patterns indicate that cylindrical shape TiO_2 is a type of directional antenna. The purpose of this study is to gain insight into the shape variation towards the antenna measurement. Therefore in this paper, DRA made of TiO_2 with high permittivity value of 84 were designed and fabricated. The structural characterization and input impedance, reflection coefficient, and radiation characteristic of the rectangular and annular DRA were investigated.

2. EXPERIMENTAL

2.1. Fabrication and Characterization

The raw material used in the present work is TiO_2 by Merck. The fabrication of the DRA can be found in [16]. The crystal structure of the sintered sample were studied by X-ray diffraction (XRD) using the Bruker D8 powder diffractometer operating in the reflection mode with Cu Kα radiation (40 kV, 30 mA) diffracted beam monochromator, using a step scan mode with the step size of 0.1° in the range of 20–65°. The morphologies of the sintered TiO_2 were characterized using a Field Emission Scanning Electron Microscope (FESEM SUPRA 35VP ZEISS) operating at working distances down to 1 mm and extended accelerating voltage range from 30 kV down to 100 V. The dielectric constant was measured using Hewlett Packard RF Impedance Analyzer 4319B. The CAD design processes are conducted by using Computer

Simulation Technology (CST) Microwave Studio while the antenna measurement was done by using Network Analyzer.

2.2. Rectangular Shape TiO$_2$ DRA Configuration

Simulated and fabricated rectangular TiO$_2$ DRA is shown in the Figure 1. In order to make comparison, the same dielectric substrate as in our previous work is used [16]. The rectangular DR of the dimension length $= 8.2$ mm, width $= 5$ mm and height $= 1$ mm is fed with a direct $50\,\Omega$ microstrip line with the same dimension as in cylindrical shape. This antenna is excited at the open-end microstrip line because at the fringing field of the line, the coupling to the antenna is at the maximum. In designing rectangular DRA, theoretical formula of conventional dielectric waveguide mode (CWDM) was used [17, 18]. The transcendental equation was solved to get k_y. By using k_y, predicted resonant frequency of DRA working at $TE_{11\delta}^Y$ can be obtained. Following separation equation is solved for f_o.

$$\varepsilon_r k_o^2 = k_x^2 + k_y^2 + k_z^2$$

Using

$$k_x = \frac{\pi}{w}, \quad k_z = \frac{\pi}{b}, \quad k_o = \frac{2\pi f_o}{c}$$

and

$$k_y \tan(k_y d/2) = \sqrt{(\varepsilon_r - 1)k_o^2 - k_y^2}$$

Where k_x and k_z is the wavenumber in the x and z direction, respectively while k_y is the wavenumber in the wave propagation as shown in the Figure 1(a). k_o is the free space wavenumber and c is the speed of light. Thus, with permittivity of 84 the theoretical resonant frequency, f_o of rectangular DRA is 8.83 GHz.

(a)   (b)
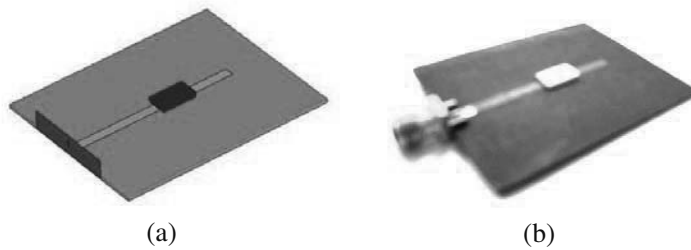
Figure 1. Geometry of the rectangular TiO$_2$ DRA (a) simulated structure, (b) fabricated structure.

(a)   (b)
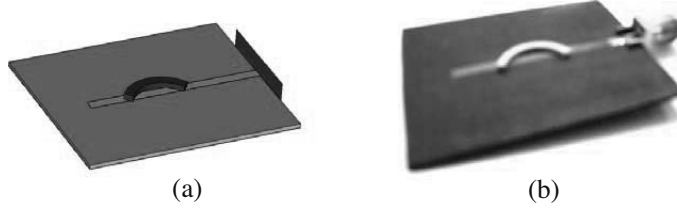
Figure 2. Geometry of the annular sector TiO$_2$ DRA for (a) simulated structure, (b) fabricated structure.

2.3. Annular Sector TiO$_2$ DRA Configuration

Geometry of the annular sector TiO$_2$ DRA is presented in the Figure 2. Outer and inner diameters of this design are 14.5 mm and 12.5 mm, respectively. The annular sector of the design is around 135°. The structure is placed 17.5 mm from the open end microstrip line to the center of the struture. Sectored-annular DRA was formed by removing a sector of a dielectric material from the circular cylindrical [19]. It is given in [19] that to predict resonant frequency of sectored-annular DRA, an approximate cavity model is used as

$$f = \frac{3 \times 10^8}{2\pi a \sqrt{\varepsilon_r}} \sqrt{X_{vp}^2 + \left[\frac{\pi a}{2d}(2m+1)\right]^2}$$

The exact value of the mode parameter v can be calculated by Equation (1) provided that the sector and inner circular surface is open faces.

$$v = \frac{n\pi}{\beta} \tag{1}$$

where $0 < \beta \leq 2\pi$ and the root X_{vp} can be found from the characteristic equation given by

$$J'_n(X_{vp}) = 0$$

Based on the value of v and X_{vp}, resonant frequency is determined.

3. RESULTS AND DISCUSSIONS

3.1. Structural Characteristic of the DRA

X-ray diffraction spectra for TiO$_2$ ceramic are presented in Figure 3. It matches the reference pattern of (21–1276) at 27.4°, 36.08°, 39.19°, 41.23°, 44.05° and 54.32°, indicating formation of crystalline rutile

phase. Figure 4 displays the representative FESEM image of the fracture surface of TiO_2 sintered at $1200°C$. The microstructure of this ceramic exhibit two different grain size, the fine grain is approximately within 0.2 to 0.5 µm and the large grain ones within 1.0 to1.5 µm.
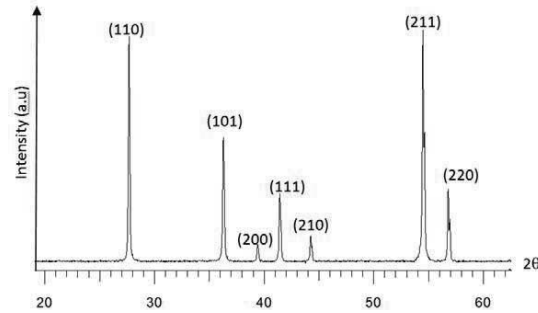
Figure 3. XRD pattern of TiO_2 at different sintering temperature $1200°C$.
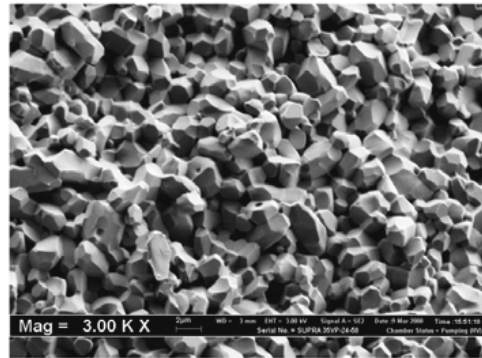
Figure 4. SEM micrograph of TiO_2 fracture surface sintered at $1200°C$.

3.2. Antenna Measurements of Rectangular Shape TiO_2 DRA

Figure 5 shows S-parameter from 8.5 GHz to 9.5 GHz in the format of Smith chart for rectangular TiO_2 DRA. The simulated minimum $|S_{11}|$ is situated on the real and imaginary parts of complex impedance, Z of 50.51 Ω and −1.545 Ω, respectively. For measured $|S_{11}|$, the complex impedance for real part is 53.84 Ω and imaginary part is −2.50 Ω. Since,

both of the input impedance is close to the center of Smith chart, therefore, this antenna experienced good impedance matching.

Figure 6 shows simulated and measured return loss for rectangular shape TiO_2 DRA. The results were viewed from 8.5 GHz to 9.5 GHz. The return loss of simulated result is -35.81 dB at 8.97 GHz while return loss for measured result is -27.49 dB at 8.92 GHz. Measured resonant frequency experiences upward shift of 50 MHz, relative to
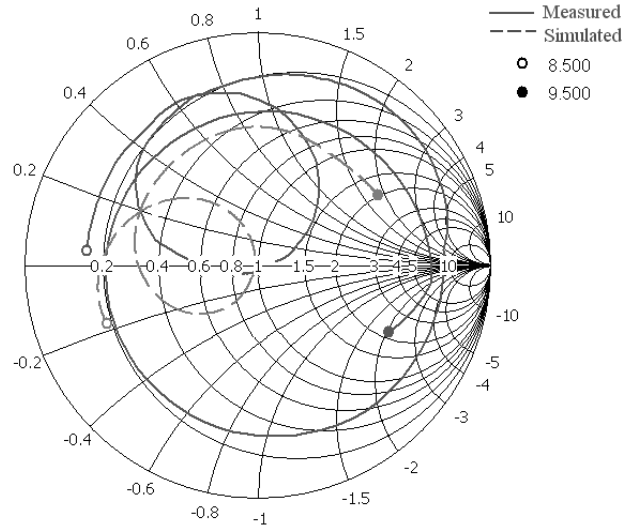
Figure 5. Smith chart for rectangular shape TiO_2 DRA.
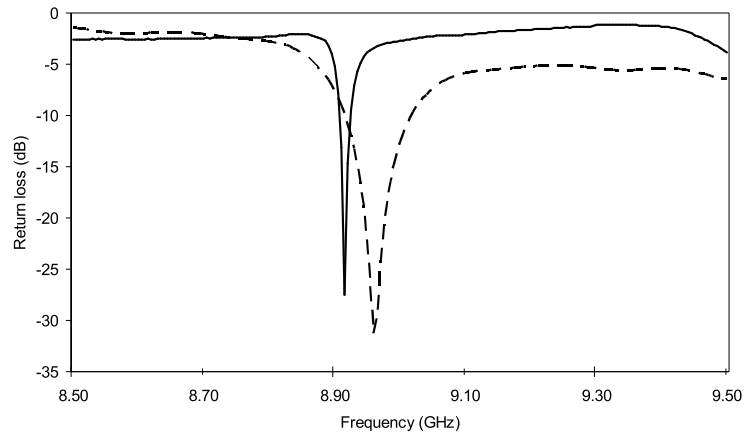
Figure 6. Return loss for rectangular shape TiO_2 DRA.

the simulated resonant frequency. Besides that, both return losses have almost the same matching level and lower than -25 dB that showed good matching level. Both curves are in good agreement. As discusses earlier in the Section 2.2, the predicted resonant frequency by using dielectric waveguide model is 8.83 GHz. By comparing with the simulated and measured results, the frequency is nearly the same. The difference between theory and experiment resonant frequency is only 90 MHz or around 1%. Simulated bandwidth at -10 dB return loss is 116 MHz whereas the measured bandwidth is lower with only 18 MHz. The measured result has a narrower bandwidth as compared to the measured one. This is due to the bad surface finishing of the rectangular dielectric resonator which tends to chip at the edge of the rectangular surface. Consequently, it affects the dielectric properties of DRA and S-parameter value.

Figure 7 shows the simulated and measured radiation patterns in E-plane for rectangular TiO_2 at 8.97 GHz and 8.92, respectively. The radiation pattern indicates one main lobe and one big back lobe. Since, the level of side lobe is a small of -10 dB, hence, this antenna pattern demonstrates that this antenna is a type of directional antenna. Comparison between measured and simulated radiation pattern shows that there are some differences between the two patterns especially at the lower half of the hemisphere where the present of the side lobes in measured radiation pattern is significant. This dissimilarity can be explained in view of the SMA connector which was connected to the DRA which may act as a significant scatterer [17]. For H-plane, both patterns are quite similar with the only difference is on the lower ground plane due to the existence of radiation from the surrounding object.

3.3. Antenna Measurements of Annular Sector TiO_2 DRA

As shown in the Figure 8, the simulated and measured input impedance for the circular shape TiO_2 DRA are plotted on the Smith chart for the frequency range of 8.5 GHz to 10 GHz. Measured input impedance is almost $50\,\Omega$ or $49.09 - j5.00\,\Omega$ since its loop almost coincide with the center of the Smith chart. It shows that maximum power transfer occurred. For the simulated input impedance, the value is only $47.07\,\Omega - j0.42\,\Omega$ since the loop move further away from the middle of the Smith chart. Hence, simulated result has better impedance matching as compared to the measured result.

Figure 9 shows the S_{11} curve for both simulated and measured result for 9 GHz to 10 GHz. Simulated return loss is lower than -10 dB with -42.26 dB at a frequency of 9.46 GHz. It is noted that measured resonant frequency shift upward to 9.50 GHz with return
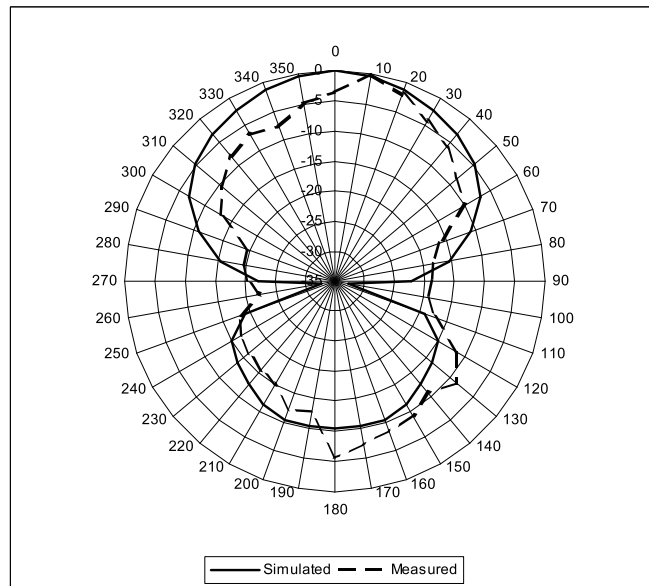
(a)
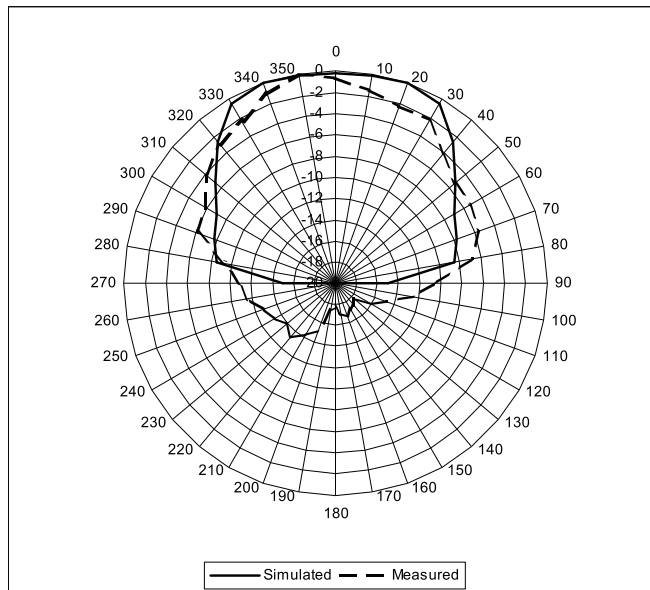
(b)

Figure 7. Radiation patterns of rectangular shape TiO_2 for (a) E-plane, (b) H-plane.

loss of 25.85 dB. The difference between the simulated and measured result is only 40 MHz or 0.4%. This indicates that both curves are in good agreement. Besides that, both return losses are lower than -25 dB that showed good matching level. In term of 10 dB return loss bandwidth, measured result has wider bandwidth of 234 MHz as compared to 182 MHz for the measurement value.

Figure 10 shows the simulated and measured E-plane and H-plane radiation patterns for annular sector shape TiO_2 at 9.483 GHz and 9.377 GHz, respectively. Here, the signal did not inclined to radiate equally in whole direction since there have dips at $90°$ and $270°$. High side lobe level of -5.8 dB associated with the finite ground plane and SMA connector can be seen from the Figure 10. Measured E-plane is not smooth as compared with simulated pattern, yet, it also has high back lobe level which indicates that this DRA is a type of bidirectional antenna. For H-plane, simulated and measured pattern is shown in the Figure 10(b) with the former one has radiation only on the upper part of the ground plane while in the latter, there is radiation also beneath the ground plane.
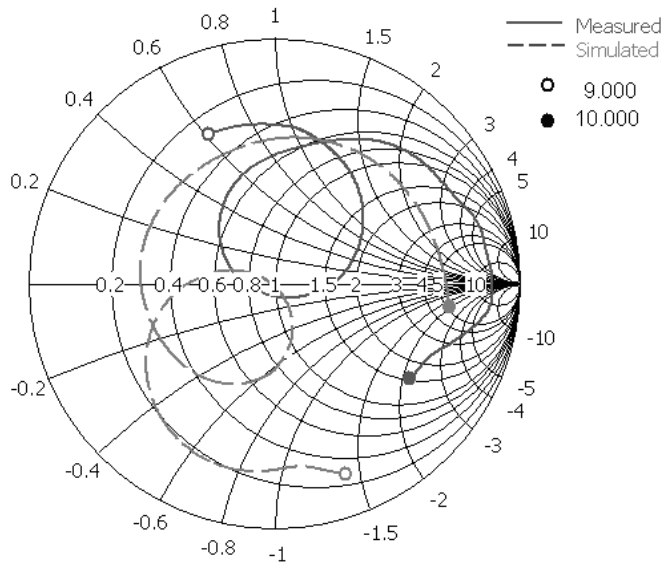
Figure 8. Smith chart for annular shape TiO_2 DRA.
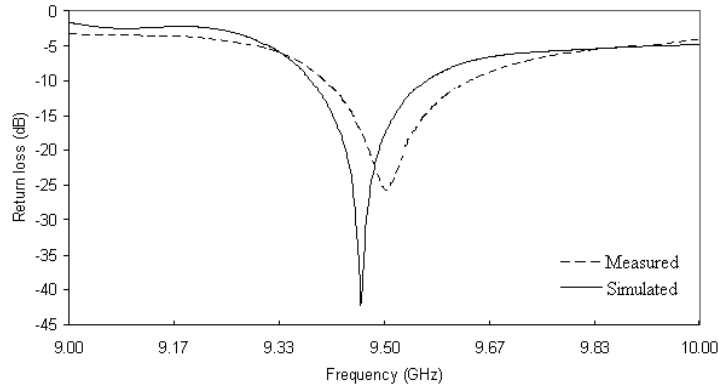
Figure 9. Return loss for annular sector TiO$_2$ DRA.

3.4. Comparison between Different Shapes TiO$_2$

As for comparison purposes we have included the measurement of cylindrical shape in this section. Figure 11 represent impedance circles of the three different shape of TiO$_2$ dielectric resonator and it was found the circles moved closer to the middle of the Smith chart indicating good match of the DRA. One can note that the measured minimum $|S_{11}|$ is not located exactly $50\,\Omega$ resistance and null reactance curve of Smith chart but from the result of all the design have good matching with the transmission line. Of the there shapes, annular sector and rectangular shape TiO$_2$ have the same level of matching with measured input impedance are $j0.42\,\Omega$ and $47.8 - j2.50\,\Omega$, respectively. The worst belonged to the cylindrical shape. Its input impedance is only $46.6 + j2.05\,\Omega$ associated with the impedance loop tend to move farther from the middle of the Smith chart.

Figure 12 shows measured return loss between cylindrical, rectangular and annular shape TiO$_2$ DRA. It is clearly can be seen that the shape of the resonator influences the resonant frequency of the DRA. In this design, three different resonators in the form of cylindrical, rectangular and annular shapes were used and resonates at three different frequencies which is accordance to the Kishk [11] and Rezaei et al. [18] Annular sector shape has the highest resonant frequency following by rectangular and cylindrical shape. The highest resonant frequency is at 9.5 GHz while the lowest belong to the cylindrical shape at 8.1 GHz. In term of return loss, all the shapes have return loss lower than -25 dB which indicate good impedance matching of the DRA. Among these three shapes, cylindrical shape
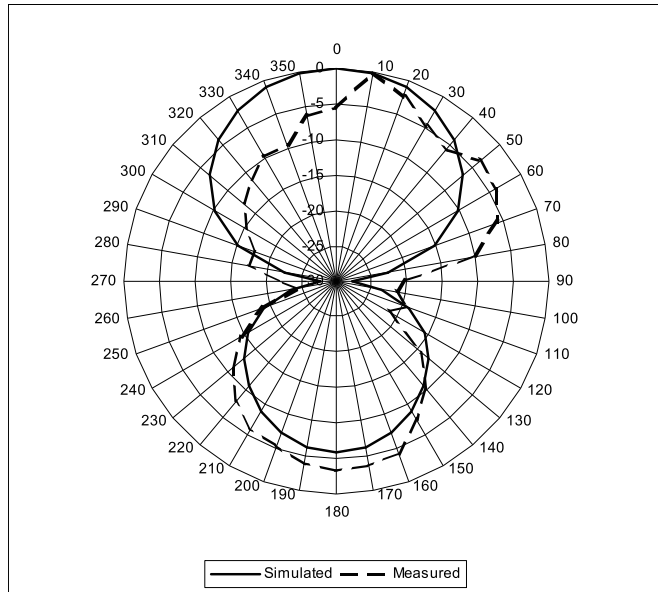
(a)
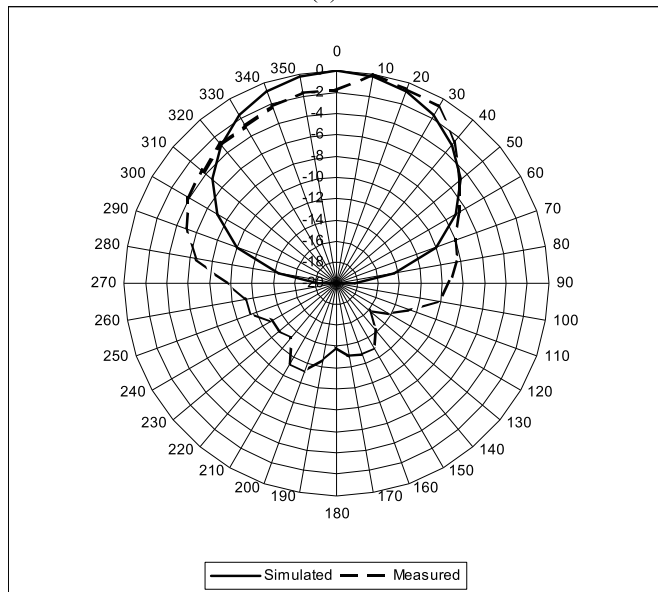
(b)

Figure 10. Radiation patterns of annular sector TiO_2 for (a) E-plane, (b) H-plane.

DRA has the lowest return loss of $-28.05\,$dB. In term of bandwidth, annular sector and rectangular DRA have the highest and lowest bandwidth $234\,$MHz and $18\,$MHz, respectively. Both rectangular and cylindrical shape DRA have narrow bandwidth with the latter one has bandwidth of only $30\,$MHz. Figure respectively.
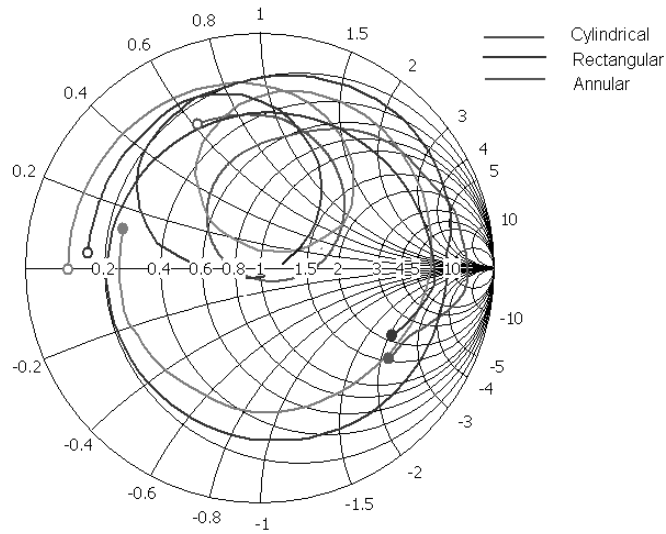
Figure 11. Measured input impedance of cylindrical, rectangular and annular shape TiO_2 DRA.
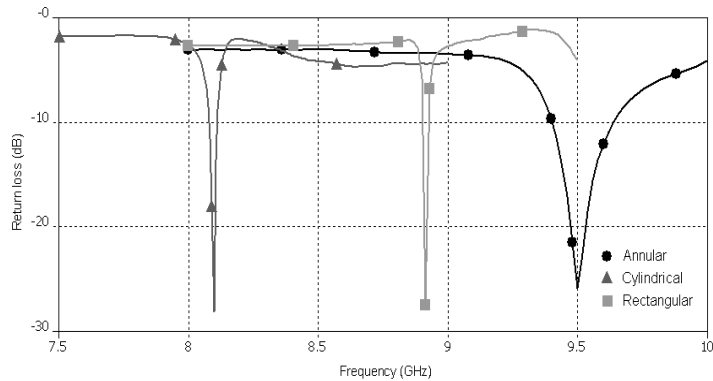
Figure 12. Measured return loss between cylindrical, rectangular and annular shape TiO_2 DRA.

Figure 13 and Figure 14 show simulated radiation pattern for each TiO_2 shape for E-plane and H-plane. The patterns are taken at their respective resonant frequencies for which the maximum power is the highest. E-plane pattern in the Figure 13 indicate that every shapes exhibit back lobe radiation with the largest one is the annular sector TiO_2 with the side lobe level of $-5.8\,dB$. Radiation pattern for the rectangular and annular shape TiO_2 proves that both are directional type antenna. However, E-plane pattern for the cylindrical sector DRA is slightly different from other shapes since cylindrical TiO_2 DRA iis lower and more power concentrate in a $0°$ direction. For H-plane field pattern, the only differences among these shapes are the scalloping and roll-off near $90°$ and $270°$ whiles no radiations occur beneath the ground plane. Therefore, it is clear from the Figure 13 and Figure 14 that there have three different radiation patterns for different shape of dielectric resonator. Event though, the difference is not significant but it is the evidence that the shape of the resonator is an important parameter in deciding the radiation pattern of the DRA.
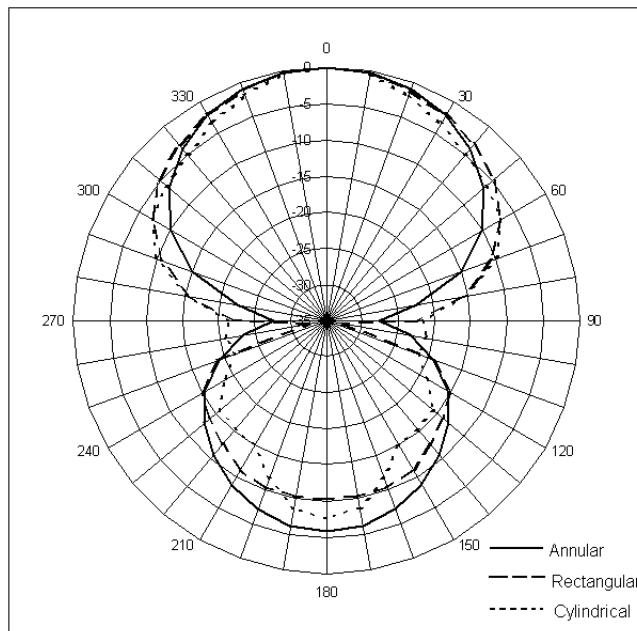
Figure 13. Simulated E-plane of cylindrical, rectangular and annular shape TiO_2 DR.
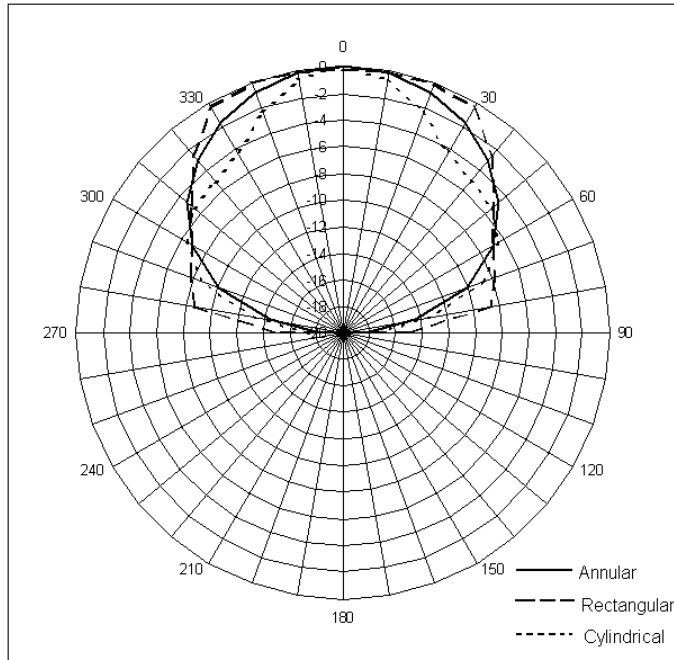
Figure 14. Simulated H-plane of cylindrical, rectangular and annular shape TiO$_2$ DRA.

4. CONCLUSION

Experimental study on rectangular, annular and cylindrical DRA excited by microstrip transmission line has been carried out and presented. All the design has good matches with the transmission line. Most of the simulated and measured results are in good agreement. It was found the shape of the resonator influences resonant frequency of the DRA. The results also prove that different geometries of DRA produce different radiation characteristics. The E-plane radiation patterns indicate that annular and rectangular shape TiO$_2$ is a type of bi-directional antenna while cylindrical DRA is a directional type antenna. It is proven that, DRA offer extra degree of freedom in designing antenna by having more geometric parameter of the structure.

REFERENCES

1. Higuchi, Y. and H. Tamura, "Recent progress on the dielectric properties of dielectric resonator materials with their applications from microwave to optical frequencies," *Journal of the European Ceramic Society*, Vol. 23, 2683–2688, 2003.

2. Huang, Y. C., M. C. Wu, T. H. Chang, J. F. Kiang, and W. F. Su, "Broadband DR antenna made of high-Q ceramic," *Journal of the European Ceramic Society*, Vol. 27, 2841–2844, 2007.

3. Ain, M. F., S. I. S. Hassan, J. S. Mandeep, M. A. Othman, B. M. Nawang, S. Sreekantan, S. D. Hutagalung, and Z. A. Ahmad, "2.5 GHz $BaTiO_3$ dielectric resonator antenna," *Progress In Electromagnetics Research*, PIER 76, 201–210, 2007.

4. De Young, C. S. and S. A. Long, "Wideband cylindrical and rectangular dielectric resonator antennas," *IEEE Antennas and Wireless Propagation Letters*, Vol. 5, No. 1, 426–429, 2006.

5. Guha, D. and Y. M. M. Antar, "New half-hemispherical dielectric resonator antenna for broadband monopole-type radiation," *IEEE Transactions on Antennas and Propagation*, Vol. 54, No. 12, 3621–3628, 2006.

6. Kishk, A., H. A. Auda, and B. C. Ahn, "Radiation characteristics of cylindrical resonant antenna with new applications," *IEEE Antennas and Propagation Society Newsletter*, Vol. 31, No. 1, 7–16, 1989.

7. Larsen, N. V. and O. Breinbjerg, "Analysis of circularly polarized hemispheroidal dielectric resonator antenna phased arrays using the method of auxiliary sources," *IEEE Transactions on Antennas and Propagation*, Vol. 55, No. 8, 2163–2173, 2007.

8. Kishk, A. A., A. W. Glisson, and G. P. Junker, "Bandwidth enhancement for split cylindrical dielectric resonator antennas," *Journal of Electromagnetic Waves and Applications*, Vol. 15, No. 6, 777–778, 2001.

9. Kishk, A. A., Y. Yin, and A. W. Glisson, "Conical dielectric resonator antennas for wideband applications," *IEEE Transactions on Antennas and Propagation*, Vol. 50, 469–474, April 2002.

10. Kishk, A. A., H. A. Auda, and B. C. Ahn, "Radiation

characteristics of cylindrical dielectric resonator antennas with new applications," *IEEE Antennas Propag. Mag.*, Vol. 31, No. 1, 7–16, 1989.

11. Kishk, A. A., "Dielectric resonator antenna, a candidate for radar applications," *IEEE Radar Conference, 2003*, 258–264, Huntsville, Alabama, 2003.

12. Junker, G. P., A. A. Kishk, and A. W. Glisson, "Input impedance of dielectric resonator antennas excited by a coaxial probe," *IEEE Transactions on Antennas and Propagation*, Vol. 42, 960–966, 1994.

13. Petosa, A., R. Larose, A. Ittipiboon, and A. Cuhaci, "Microstrip fed array of multisegment dielectric resonator antennas," *IEE Proc.-Microwave Antennas Propag.*, Vol. 144, 472–476, 1997.

14. Mridula, S., S. K. Menon, P. Mohanan, P. V. Bijumon, and M. T. Sebastian, "Characteristics of a microstrip excited high-permittivity rectangular dielectric resonator antenna," *Microwave Optical Technol. Lett.*, Vol. 40, No. 4, 316–318, 2004.

15. Malekabadi, S. A. and M. H. Neshati, "Circular polarized dielectric resonator antennas using a single probe feed," *Progress In Electromagnetics Research C*, Vol. 3, 81–94, 2008.

16. Sreekantan, S., Y. K. Ling, Z. A. Ahmad, M. F. Ain, S. I. S. Hassan, and M. A. Othman, "Structural characterization and performance of dielectric antenna made of TiO_2," sumbitted to *Journal European Ceramic Society*.

17. Antar, Y. M. M., "New directions in antenna research using dielectrics," *Radio Science Conference, 2003. 1RSC 2003. Proceedings of the Twentieth Lational*, 1–11, Cairo, Egypt, 2003.

18. Kumar Mongia, R. and A. Ittipiboon, Theoretical and experimental investigations on rectangular dielectric resonator antennas," *Antennas and Propagation, IEEE Transactions on*, Vol. 45, No. 9, 1348–1356, 1997.

19. Tam, M. T. K. and R. D. Murch, "Compact circular sector and annular sector dielectric resonator antennas," *IEEE Transactions on Antennas and Propagation*, Vol. 47, No. 5, 837–842, 1999.

20. Petosa, A., *Dielectric Resonator Antenna Handbook*, Artech House, Bolton, 2007.

21. Rezaei, P., M. Hakkak, and K. Forooraghi, "Design of wideband dielectric resonator antenna with a two-segment structure," *Progress In Electromagnetics Research*, PIER 66, 111–124, 2006.